PAPER

Architectural diversity in the solid-state behaviour of crown ether and [2.2.2]-cryptand complexes of K⁺TCNQ·⁻ salts†

Bingjia Yan,‡[a] Peter N. Horton,[a] Simon C. Weston, ID §[a] Christopher J. Wedge, ID [b] Andrea E. Russell ID [a] and Martin C. Grossel ID *[a]

The solid-state behaviour of five ionophore-encapsulated TCNQ complexes: (18-crown-6)K(TCNQ)$_{2.5}$ (**1**), ([2.2.2]-cryptand)K(TCNQ)$_{2.5}$ (**2**), (benzo-18-crown-6)K(TCNQ)$_2$ (**3**), (dibenzo-18-crown-6)K(TCNQ)$_2$ (**4**), and (dicyclohexano-18-crown-6)K(TCNQ)$_3$ (**5**) has been explored. For both **1** and **2**, the TCNQ components assemble as a pentameric repeat unit within infinite TCNQ columns with the cation complex sitting in a cavity between the columns; whereas for **3** and **4**, neighbouring (crown ether)K⁺ complexes form dimers involving K⁺–π interactions which further assemble into one-dimensional columns sitting between infinite TCNQ stacks. In the solid-state complex **5**, the crown ether adopts a chair conformation with the resulting (crown ether)K⁺ complex assembling into a one-dimensional ladder. Pairs of TCNQ dimers separated by an isolated TCNQ unit form infinite TCNQ columns. IR and Raman spectroscopy reveal the presence of partially charged TCNQ units within all five TCNQ complexes (**1–5**) and resistivity studies indicate that all five TCNQ complexes (**1–5**) are more conductive than the corresponding simple KTCNQ salts. Preliminary EPR studies of **1** and **2** indicate typical behaviour of complex TCNQ salts (containing both TCNQ⁰ and TCNQ·⁻).

Introduction

We have previously demonstrated the ability of crown-ether complexation to control the solid-state architecture and hence electronic properties of metal TCNQ·⁻ salts in the solid-state.[1–7] In this paper, we report the impact of various macrocyclic hosts on the solid-state behaviour of potassium TCNQ salts [K⁺ TCNQ·⁻, K⁺(TCNQ)$_2$·⁻, K⁺(TCNQ)$_{2.5}$·⁻, and K⁺(TCNQ)$_3$·⁻]. Whilst the K⁺ cation can sit comfortably within the cavity of 18-crown-6,[8–10] several other two-dimensional analogues of 18-crown-6 moieties, *e.g.* benzo-18-crown-6,[11] dibenzo-18-crown-6,[11] and dicyclohexano-18-crown-6 (ref. 12) have also demonstrated the ability to complex the K⁺ cation {see for example [K(benzo-18-crown-6)]NCS,[11] [K(dibenzo-18-crown-6)]$_2$[Hg(SCN)$_4$],[11] and [K(dicyclohexano-18-crown-6)][2-

nitrophenoxide]}.[12] The K⁺ cation can also fit well into the cavity of 2.2.2-cryptand where it is completely screened from direct interaction with counter-ions.[13–15] A key feature of the solid-state behaviour of TCNQ·⁻ salts is the ability of this anion to form face-to-face π-stacked dimers and infinite stacks, which show a variety of electronic properties.[3,7,16–19]

We have previously described the solid-state behaviour of KTCNQ complexes with 18-crown-6[3–5] and 15-crown-5,[1] respectively. We now report the impact of complexation with other two- and three-dimensional ionophores on its solid-state behaviour, including (18-crown-6)K(TCNQ)$_{2.5}$ (**1**), ([2.2.2]-cryptand)K(TCNQ)$_{2.5}$ (**2**), (benzo-18-crown-6)K(TCNQ)$_2$ (**3**), (dibenzo-18-crown-6)K(TCNQ)$_2$ (**4**), and (dicyclohexano-18-crown-6)K(TCNQ)$_3$ (**5**). Fig. 1 summarises the five TCNQ complexes (**1–5**) discussed in this study together with two reference TCNQ salts, which we have previously investigated (**6** and **7**).

Experimental

General details

All experiments were performed under a nitrogen protective environment unless stated otherwise. Acetonitrile (MeCN) was dried over calcium hydride and distilled before use. Diethyl ether (Et$_2$O) was dried over sodium wire and was freshly decanted before use. Dichloromethane (DCM) was

[a] School of Chemistry, University of Southampton, Highfield, Southampton, SO17 1BJ, UK. E-mail: M.C.Grossel@soton.ac.uk; Fax: +44 (0)23 8059 3781; Tel: +44 (0)23 8059 3153
[b] Department of Chemical Sciences, University of Huddersfield, Huddersfield, HD1 3DH, UK

‡ Current address: Leibniz-Forschungsinstitut für Molekulare Pharmakologie, 13125 Berlin, Germany.
§ Current address: ExxonMobil Technology & Engineering Company, Annandale, NJ 08801, USA.
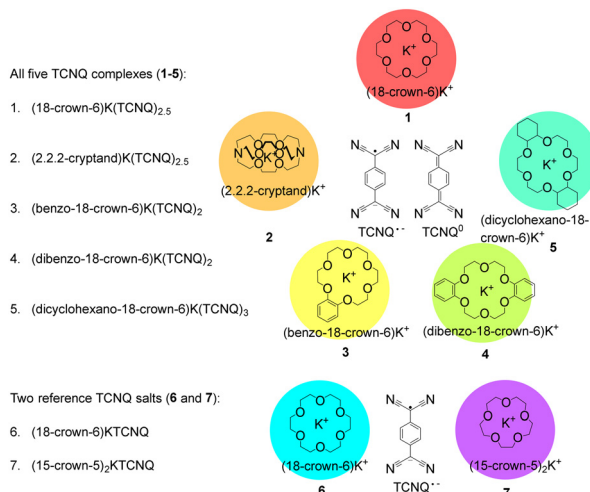
Paper

Fig. 1 Structures of all the TCNQ complexes (**1**–**5**) along with the two reference TCNQ salts (**6** and **7**).

dried over calcium hydride and distilled before use. All chemicals were commercially available and used as received unless otherwise stated.

Instrumentation

Melting points were measured on an Electro-thermal melting point apparatus and are uncorrected. Elemental analyses were performed by Medac Ltd., Chobham Business Centre, Chertsey Road, Chobham, Surrey, GU24 8JB. Infrared spectroscopy (IR) (KBr discs) spectra were obtained using a Golden Gate sampling attachment on a Mattson Satellite 3000 FTIR instrument. Raman Spectra were collected using a Renishaw In-Via system with a high powered near Infrared (HPNIR) 785 nm laser and microscope using a 50× objective. ESI mass spectra were obtained using a solariX (Bruker Daltonics, Bremen, Germany) mass spectrometer equipped with a 4.7T magnet and FT-ICR cell. Resistance data were recorded by MASTECH MY64 digital multimeter AC/DC voltage current resistance tester detector with diode.

Single crystal X-ray crystallography

A suitable crystal was selected and measured following a standard method[20] for each compound. **1**–**3**, **5** using a *Rigaku AFC12* goniometer equipped with an enhanced sensitivity (HG) *Saturn724+* detector mounted at the window of a *FR-E+ SuperBright* molybdenum rotating anode generator with HF *Varimax* optics (100 μm focus) at 100 K. **4** on a *Rigaku SPIDER RAPID* diffractometer at 120 K with an image plate detector. Cell determination and data collection were carried out using *CrstalClear*.[21] Data reduction, cell refinement and absorption correction were carried out using either *CrystalClear*[21] (**4**) or *CrysAlisPro*[22] (**1**–**3**, **5**). Structures were solved with Olex2 (ref. 23) using *ShelXT*[24] and refined using *ShelXL*.[25]

Electron paramagnetic resonance

All of the measurements were performed at X-band (~9.5 GHz) on a Bruker EMX EPR spectrometer equipped with a programmable goniometer (ER 218PG1) and using standard resonators (Bruker ER 4122 SHQE unless otherwise stated). Temperature control was achieved using nitrogen gas flow from a B-VT 2000 temperature controller with a quartz dewar insert (ER 169DIS). Microwave power was optimised to ensure signal response in the linear regime, typically requiring <1 mW. The presence of distinct species giving rise to signals of vastly different intensity and linewidth necessitated deliberate over-modulation of the narrower line for some samples.

Typical procedure for the preparation of KTCNQ-ionophore complexes

A solution of KTCNQ (0.1 mmol), with or without TCNQ^0 (0.1 mmol), and the ionophore (0.1 mmol) in dry acetonitrile (50 ml) was heated under reflux for 3 hours. The solution was then filtered whilst hot and left to cool. The solvent was allowed to evaporate slowly over a period of several days and the resulting solid was then separated by filtration, washed with dry diethyl ether (50 ml) and dried in vacuum to afford crystals of the ionophore complex.

Preparation of (18-crown-6)K(TCNQ)$_{2.5}$ (1)

Reaction of KTCNQ (0.0243 g, 0.1 mmol), TCNQ^0 (0.0204 g, 0.1 mmol) and 18-crown-6 (0.0264 g, 0.1 mmol) in dry acetonitrile (50 ml) afforded needles of a bright black crystalline solid **1** (0.0431 g, 61%). MS (solution) (MeCN) (ESI$^-$) m/z: 204.1 (TCNQ$^{\cdot-}$). (ESI$^+$) m/z: 287.2 (Crown + Na$^+$). IR v_{max}/cm^{-1} 2899 (saturated $\underline{CH}$ stretch), 2209, 2196, 2176 ($\underline{C{\equiv}N}$ stretch), 1566 ($\underline{C{=}C}$(CN)$_2$ stretch), 1522 ($\underline{C{=}C}$ ring stretch), 1341 ($\underline{CH}$ bend), 1159 ($\underline{C{-}CN}$ and $\underline{C{-}C}$ ring stretch), 961 ($\underline{C{-}C}$ ring stretch), 839, 700 ($\underline{CH}$ out of plane bend). Raman v_{max}/cm^{-1} 2203 ($\underline{C{\equiv}N}$ stretch), 1603 ($\underline{C{=}C}$ ring stretch), 1386 ($\underline{C{-}CN}$ stretch), 1204 (C$=$$\underline{C}$-H bending). M.p. 256 °C (dec.). Elemental analysis: calculated: C: 61.98%, H: 4.21%, N: 17.21%. Found: C: 61.84%, H: 4.00%, N: 17.08%.

Preparation of ([2.2.2]-cryptand)K(TCNQ)$_{2.5}$ (2)

Reaction of KTCNQ (0.243 g, 1 mmol), TCNQ^0 (0.204 g, 1 mmol) and [2.2.2]-cryptand (0.377 g, 1 mmol) afforded small crystals of **2** as a bright black crystalline solid (0.4002 g, 49%). MS (solution) (MeCN) (ESI$^-$) m/z: 204.1 (TCNQ$^{\cdot-}$). (ESI$^+$) m/z: 399.2 (crown + Na$^+$). IR v_{max}/cm^{-1} 2956, 2890, 2823 (saturated $\underline{CH}$ stretch), 2196, 2178 ($\underline{C{\equiv}N}$ stretch) (lit.[26] 2177, 2156), 1565 ($\underline{C{=}C}$(CN)$_2$ stretch), 1525 ($\underline{C{=}C}$ ring stretch), 1355 ($\underline{CH}$ bend), 1106 ($\underline{C{-}CN}$ and $\underline{C{-}C}$ ring stretch), 941 ($\underline{C{-}C}$ ring stretch), 842, 749 ($\underline{CH}$ out of plane bend). Raman v_{max}/cm^{-1} 2189 ($\underline{C{\equiv}N}$ stretch), 1614, 1600 ($\underline{C{=}C}$ ring stretch), 1434, 1389 ($\underline{C{-}CN}$ stretch), 1195 (C$=$$\underline{C}$-H bending). M.p. 210 °C (dec.). Elemental analysis: calculated: C: 62.25%, H: 5.01%, N: 18.15%. Found: C: 62.18%, H: 5.02%, N: 18.06%.

Preparation of (benzo-18-crown-6)K(TCNQ)₂ (3)

Reaction of KTCNQ (0.0243 g, 0.1 mmol), TCNQ⁰ (0.0204 g, 0.1 mmol) and benzo-18-crown-6 (0.0312 g, 0.1 mmol) afforded small crystals of **3** as dark blue needles (0.0433 g, 57%). These small crystals of **3** were then re-crystallized from hot dry DCM in order to remove residual MeCN. MS (solution) (MeCN) (ESI⁻) *m/z*: 204.1 (TCNQ˙⁻). (ESI⁺) *m/z*: 335.2 (Crown + Na⁺). IR v_{max}/cm⁻¹ 3052, 2937 (saturated C$\underline{\text{H}}$ stretch), 2226, 2195, 2166 (C$\equiv$N stretch), 1559 (C$=$C(CN)₂ stretch), 1507 (C$=$C ring stretch), 1301 (C$\underline{\text{H}}$ bend), 1120 (C–CN and C–C ring stretch), 937 (C–C ring stretch), 830, 684 (C$\underline{\text{H}}$ out of plane bend). Raman v_{max}/cm⁻¹ 2207 (C$\equiv$N stretch), 1606 (C$=$C ring stretch), 1390 (C–CN stretch), 1205 (C$=$C–H bending). M.p. 200 °C (dec.). Elemental analysis: calculated: C: 63.40%, H: 3.99%, N: 14.78%. Found: C: 62.88%, H: 3.70%, N: 15.02%.

Preparation of (dibenzo-18-crown-6)K(TCNQ)₂ (4)

Reaction of KTCNQ (0.0243 g, 0.1 mmol), TCNQ⁰ (0.0204 g, 0.1 mmol) and dibenzo-18-crown-6 (0.0360 g, 0.1 mmol) gave **4** (0.0565 g, 70%) as black crystals. MS (solution) (MeCN) (ESI⁻) *m/z*: 204.1 (TCNQ˙⁻). (ESI⁺) *m/z*: 383.2 (crown + Na⁺). IR v_{max}/cm⁻¹ 2968, 2935, 2887 (saturated C$\underline{\text{H}}$ stretch), 2214, 2189 (C$\equiv$N stretch), 1579 (C$=$C(CN)₂ stretch), 1528 (C$=$C ring stretch), 1379 (C$\underline{\text{H}}$ bend), 1161 (C–CN and C–C ring stretch), 948 (C–C ring stretch), 815, 709 (C$\underline{\text{H}}$ out of plane bend). Raman v_{max}/cm⁻¹ 2204 (C$\equiv$N stretch), 1605 (C$=$C ring stretch), 1388 (C–CN stretch), 1205 (C$=$C–H bending). M.p. 220 °C (lit.[27] 224–225 °C). Elemental analysis:[28] calculated: C: 65.42%, H: 3.99%, N: 13.87%. Found: C: 65.18%, H: 3.92%, N: 13.91%.

Preparation of (dicyclohexano-18-crown-6)K(TCNQ)₃ (5)

Reaction of KTCNQ (0.0243 g, 0.1 mmol), TCNQ⁰ (0.0204 g, 0.1 mmol) and dicyclohexano-18-crown-6 (0.0372 g, 0.2 mmol) formed small crystals of **5** as small bright purple crystalline needles (0.0516 g, 63%). MS (solution) (MeCN) (ESI⁻) *m/z*: 204.1 (TCNQ˙⁻). (ESI⁺) *m/z*: 395.2 (crown + Na⁺). IR v_{max}/cm⁻¹ 2932, 2883 (saturated C$\underline{\text{H}}$ stretch), 2222, 2201, 2174 (C$\equiv$N stretch), 1559 (C$=$C(CN)₂ stretch), 1507 (C$=$C ring stretch), 1330 (C$\underline{\text{H}}$ bend), 1125 (C–CN and C–C ring stretch), 950 (C–C ring stretch), 841, 749 (C$\underline{\text{H}}$ out of plane bend). Raman v_{max}/cm⁻¹ 2203 (C$\equiv$N stretch), 1605 (C$=$C ring stretch), 1389 (C–CN stretch), 1204, 1195 (C$=$C–H bending). M.p. 228 °C (dec.). Elemental analysis: calculated: C: 65.67%, H: 4.72%, N: 16.41%. Found: C: 65.85%, H: 4.79%, N: 16.66%.

Results and discussion

Crystallization of KTCNQ from anhydrous acetonitrile in the presence of crown ether (18-crown-6, benzo-18-crown-6, dibenzo-18-crown-6, dicyclohexano-18-crown-6) or [2.2.2]-cryptand and one molar equivalent of TCNQ⁰ afforded the corresponding crystals of (18-crown-6)K(TCNQ)₂.₅ (**1**), ([2.2.2]-cryptand)K(TCNQ)₂.₅ (**2**), (benzo-18-crown-6)K(TCNQ)₂ (**3**), (dibenzo-18-crown-6)K(TCNQ)₂ (**4**), and (dicyclohexano-18-crown-6)K(TCNQ)₃ (**5**), which proved suitable for single crystal X-ray structural study.

The solid-state behaviour of TCNQ complexes (1 and 2)

(18-Crown-6)K(TCNQ)₂.₅ (**1**) crystallized in the monoclinic space group $P2_1/c$. The asymmetric unit contains one cation disc of (18-crown-6)K⁺ in combination with two and a half TCNQ species (TCNQ-A, blue/ TCNQ-B, red/TCNQ-C, green). Each K⁺ moiety is sitting in the 18-crown-6 cavity and is coordinated to two TCNQ units (TCNQ-A and TCNQ-C) at each face of the (18-crown-6)K⁺ complex with the corresponding K⁺···NC contact distances of 2.809(1) Å (K⁺···$_A$NC, TCNQ-A) and 2.882(1) Å (K⁺···$_C$NC, TCNQ-C). The coordination angle CN$_A$···K⁺···$_C$NC is 163.17° (see Fig. 2).

The three crystallographically inequivalent TCNQ moieties namely, TCNQ-A (blue), TCNQ-B (red), and TCNQ-C (green) form a pentamer repeat unit, in which the individual TCNQ components are π-stacked and alternately long and short-axis slipped (see Fig. 3).

Specifically, TCNQ-B adopts a shallow chair conformation with the two terminal groups of –C(C$\equiv$N)₂ bending (3.76°) away from the central benzene ring, whereas TCNQ-A forms a shallow boat conformation, in which one terminal –C(C$\equiv$N)₂ moiety is rotated (by 2.99°) and the other –C(C$\equiv$N)₂ unit is bent (by 0.87°) with respect to the central aromatic ring. TCNQ-C adopts a nearly planar conformation with one terminal –C(C$\equiv$N)₂ group rotated in a manner similar to that seen for TCNQ-A but with the corresponding angles of 2.63° and 3.01° instead (see Fig. 4). Within each TCNQ pentamer, a dimer pair of TCNQ-A/C is significantly long-axis slipped. In contrast, short-axis slippage is seen in the dimer pair TCNQ-A/B and between neighboring TCNQ pentamers (TCNQ-CC′) (see Fig. S1 and Table S2† for the key structural features).

From a consideration of the length of the external bond (C–C in TCNQ˙⁻ and C$=$C in TCNQ⁰), which connects the –C(C$\equiv$N)₂ substituent to the central aromatic ring on each TCNQ unit, it seems that TCNQ-A has more TCNQ˙⁻ character (because this bond-length in TCNQ-A is significantly longer [1.403(2) Å] than the corresponding bond-length in either TCNQ-B [1.378(2) Å] or TCNQ-C [1.390(2)/1.392(2) Å]). However, because of the tendency for the formation of
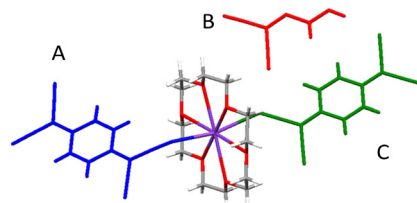

Fig. 2 Asymmetric unit of (18-crown-6)K(TCNQ)₂.₅ (**1**) in this study. All the TCNQ units (TCNQ-A/B/C) have been coloured separately in order to distinguish their crystallographic inequivalence (*n.b.* fragment B is one half of a TCNQ unit).
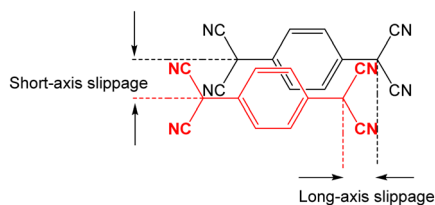
Fig. 3 Definition of long- and short-axis slip distances between neighbouring TCNQ units in this study.
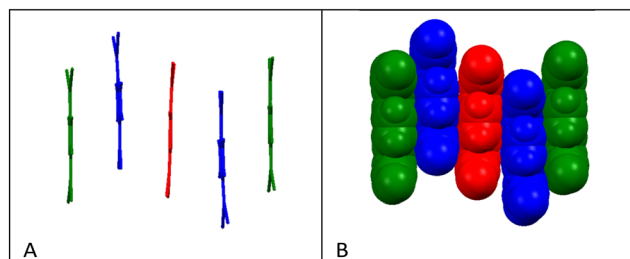

Fig. 4 Capped stick (A) and space-filling (B) diagrams of TCNQ pentamer stack in (18-crown-6)K(TCNQ)$_{2.5}$ (**1**).

mixed-valence TCNQ dimers,[29] two electrons are delocalized over the five TCNQ units but more negative charge density appears to reside on the second and fourth TCNQ-A units. Within each pentamer, the interplanar distances between the neighbouring TCNQ units [3.17 Å (TCNQ-AC), 3.38 Å (TCNQ-AB); and 3.35 Å (TCNQ-CC′)] suggest strong π–π interactions between each of the TCNQ units.

This pentamer unit (···CABA′C′···) further assembles into infinite face-to-face π-stacked TCNQ columns with the cation disc (18-crown-6)K$^+$ located in the cavities present on both sides of the infinite TCNQ columns, there being two cation complexes associated with opposite sides of each pentamer unit, and rotated with respect to each other by 85.64° (mean plane set by 18-crown-6 oxygen atoms, see Fig. 5A and B). Additionally, neighbouring TCNQ pentamers form a herringbone-packing pattern (see Fig. 5C and D).
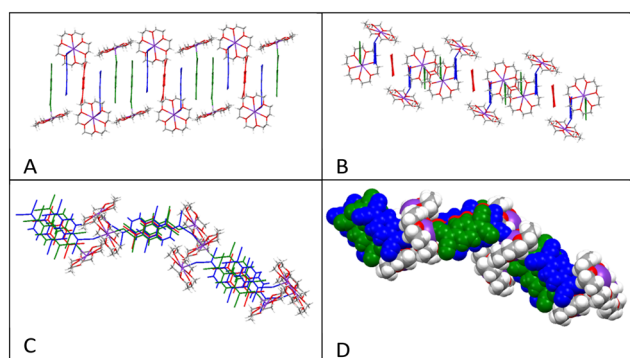
This unusual stoichiometry [1 : 2.5 or 2 : 5, (18-crown-6)K$^+$: TCNQ] has also been reported for (n-Bu$_4$N)$_2$(TCNQ)$_5$ by Martin and co-workers[16] where the asymmetric unit contains one n-Bu$_4$N$^+$ cation and two and a half TCNQ units. Each TCNQ column is separated by n-Bu$_4$N$^+$ cations in a layer with C–H "hydrogen bonds" between the cyano groups of the TCNQ moieties and the CH$_2$ groups from the corresponding n-Bu$_4$N$^+$ counter-cations.[16]

The ([2.2.2]-cryptand)K(TCNQ)$_{2.5}$ salt (**2**) shows similar solid state behaviour, but in this case the K$^+$ cation is tightly bound within the cavity of the [2.2.2]-cryptand, thereby preventing any direct contact with the cyano groups of adjacent TCNQ units. The asymmetric unit contains one cation barrel of the K$^+$[2.2.2]-cryptate, its charge being balanced by two and a half TCNQ units (see Fig. 6).

As seen in ([2.2.2]-cryptand)K(TCNQ)$_{2.5}$ (**2**) above, three crystallographically inequivalent TCNQ units, TCNQ-A (blue), TCNQ-B (red), and TCNQ-C (green) are face-to-face π-stacked and show alternating long- or short-axis slippage (see Table S2†) for the key structural features), resulting in the formation of a pentamer packing motif of ···CABA′C′··· (see Fig. 7). Within each TCNQ pentamer, both TCNQ-A and TCNQ-C adopt a shallow boat conformation, in which neighbouring –C(C≡N)$_2$ moieties on each TCNQ unit are twisted away from each other (see Fig. S2A†). TCNQ-A has one terminal –C(C≡N)$_2$ moiety significantly bent away (by 3.54°) from the central aromatic ring. TCNQ-B is nearly planar (see Fig. 7 and S2C†). In TCNQ-C, both of the terminal groups –C(C≡N)$_2$ are rotated (by 2.71° and 1.43°) with respect to the aromatic-ring core (see Fig. S2E†).

Both of the dimer pairs of TCNQ-AC and TCNQ-AB are significantly long-axis slipped with respect to each other (see Fig. S2B and D†). Furthermore, within both of the TCNQ dimers, the two TCNQ planes are slightly tilted with respect to each other by ca. 4.52° in TCNQ-AC and 1.55° in TCNQ-AB, respectively. The π–π contact distances between the mean planes (defined by the central aromatic ring) of the adjacent TCNQ moieties are 3.08 Å in TCNQ-AC, 3.24 Å in TCNQ-AB, and 2.98 Å in TCNQ-CC′, respectively (see Fig. S2 and Table S2† for the key structural features). Furthermore, in both complexed salts (**1**) and (**2**) neighbouring TCNQ pentamers

Fig. 5 Capped stick side (A) and top (B) views of pentamer units and their packing motifs in (18-crown-6)K(TCNQ)$_{2.5}$ (**1**) together with the zig-zag packing arrangement formed by neighbouring TCNQ columns (C) as capped sticks, and (D) space-filled.
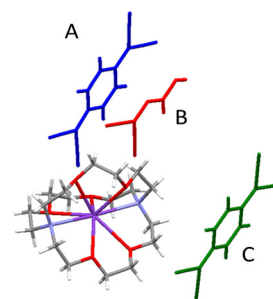

Fig. 6 Asymmetric unit of ([2.2.2]-cryptand)K(TCNQ)$_{2.5}$ (**2**) in this study. Each of the TCNQ units has been coloured separately in order to distinguish their crystallographic inequivalence.
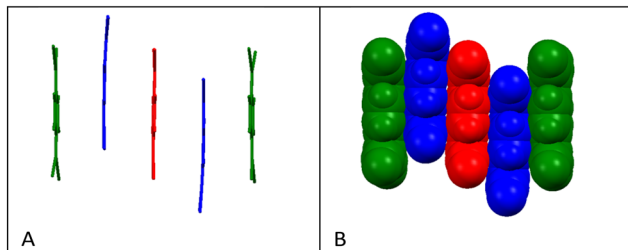
Fig. 7 Capped stick (A) and space-fill (B) diagrams of TCNQ pentamer stack in ([2.2.2]-cryptand)K(TCNQ)$_{2.5}$ (**2**).

Fig. 9 Asymmetric unit of (benzo-18-crown-6)K(TCNQ)$_2$ (**3**) in colour (the greyed atoms indicate the symmetry generated remainder of the crown ether and the other TCNQ unit).

adopt a similar "zig-zag" packing motif as observed in Fig. 5(C and D) and 8(C and D).

The TCNQ pentamer repeat unit lies between two layers of ([2.2.2]-cryptand)K$^+$ moieties and assembles into infinite wave-like TCNQ face-to-face π-stacked columns (see Fig. 8B). Two electrons are delocalized over the five TCNQ units but more negative charge density appears to reside on the second and fourth TCNQ units (TCNQ-A) as reflected in the external ring –C(C≡N)$_2$ bond lengths on each TCNQ unit. Once again, neighbouring TCNQ columns adopt a herringbone packing motif (see Fig. 8C and D) similar to that seen for **1**.

Cation–π interactions in ionophore alkali metal TCNQ complexes (3 and 4)

In (benzo-18-crown-6)K(TCNQ)$_2$ (**3**), the asymmetric unit contains half a (benzo-18-crown-6)K$^+$ complex (partly disordered) and a TCNQ moiety. Each K$^+$ cation is complexed within one crown ether unit and there is no contact with cyano groups of the TCNQ units. The K$^+$ cation sits 0.28 Å above the mean plane (as defined by six oxygen atoms) of the crown ether ring. Part of the benzo-18-crown-6 ligand is disordered as shown in Fig. 9. The phenyl ring on benzo-18-crown-6 is twisted by 6.92° with respect to the mean plane (as defined by six oxygen atoms) of 18-crown-6.
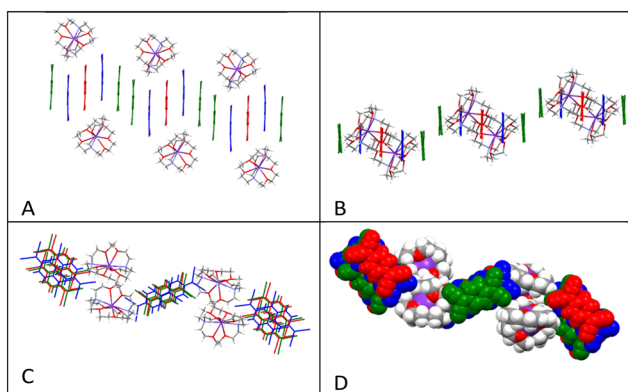
The cation complex (benzo-18-crown-6)K$^+$ assembles into a one-dimensional infinite "staircase" stacked structure linked by K$^+$–π interactions between neighbouring units (see Fig. 10A). The K$^+$–K$^+$ distance between neighbouring cations is 6.44 Å. The average vertical distance of the K$^+$ cation above the mean plane (as defined by six oxygen atoms) of the adjacent phenyl ring of the crown ether ring is 3.79 Å, resulting in long-axis slippage between neighbouring cation barrels of 5.21 Å. Each (benzo-18-crown-6)K$^+$ has an offset π-stacked geometry, which minimizes π–π repulsion between adjacent phenyl rings in a manner similar to that reported for [K(benzo-18-crown-6)]NCS.[11] However, in the latter case, neighbouring (benzo-18-crown-6)K$^+$ units form a "zig-zag" repetitive packing pattern which further assembles into a one-dimensional infinite chain instead of generating uni-directional and one-dimensional infinite columns as viewed in **3**.

The TCNQ effectively self-dimerises (A⋯A*) within extended face-to-face π-stacked columns (see Fig. 11). Within each dimer, the TCNQ units are significantly long-axis slipped with a face-to-face π–π separation of 3.18 Å (see Fig. S3 and Table S2† for the key structural features). Additionally, the TCNQ unit is essentially planar but with one terminal –C(C≡N)$_2$ moiety rotated relative to the mean plane of the central aromatic ring by 5.21°. Neighbouring TCNQ dimers interact further *via* inter-dimer interactions assembling into extended infinite TCNQ columns, ⋯(A⋯A*)⋯(A⋯A*)⋯, and form parallel (in-plane) sheets throughout the structure separated by the cation barrels of (benzo-18-crown-6)K$^+$ complexes (see Fig. 11A). The TCNQ columns consist of a 1:1 mixture of TCNQ$^{·-}$ and TCNQ^0 components, but as there is only one TCNQ moiety within the asymmetric unit, only an

Fig. 8 Capped stick side (A) and top (B) views of the pentamer geometry and packing pattern of the TCNQ columns, together with the zig-zag packing arrangement (C-capped sticks and D-space-filling) formed by neighbouring TCNQ columns in ([2.2.2]-cryptand)K(TCNQ)$_{2.5}$ (**2**).
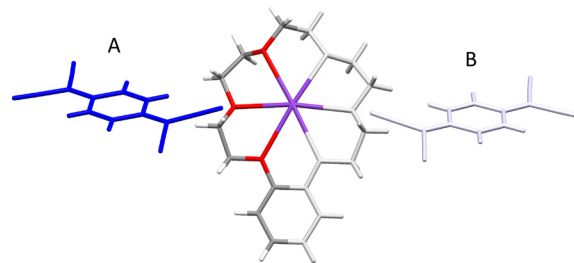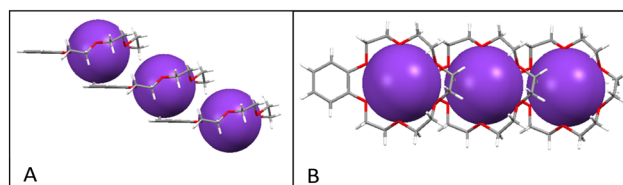
Fig. 10 Side (A) and top (B) views of the one-dimensional infinite chain structure found in the cation barrels of (benzo-18-crown-6)K$^+$ in (**3**) arising from intermolecular K$^+$–π interactions.
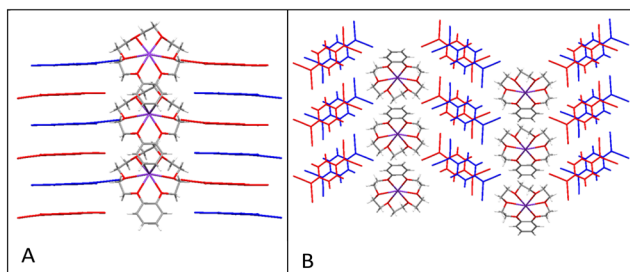
Fig. 11 Capped stick side (A) and top (B) views of the packing pattern in (benzo-18-crown-6)K(TCNQ)$_2$ (**3**) in this study (TCNQ-A in blue and TCNQ-A' in red).

average is observed. Neighbouring TCNQ columns form a "zig-zag" packing pattern as observed for **3**.

In (dibenzo-18-crown-6)K(TCNQ)$_2$ (**4**), each K$^+$ cation is complexed within one crown ether ring with no direct interactions between cyano groups on adjacent TCNQ units, in a manner similar to that seen in **3**. The asymmetric unit in **4** includes one cation barrel of (dibenzo-18-crown-6)K$^+$ and two crystallographically inequivalent TCNQ units, TCNQ-A (blue) and TCNQ-B (red) (see Fig. 12).

The dibenzo-18-crown-6 K$^+$ complex adopts a "butterfly" conformation (see Fig. 13). The angle between the mean planes of two aromatic rings is 54°. Meanwhile, both aromatic rings are bent relative to the mean plane of the central 18-crown-6 (as defined by the six oxygen atoms) at angles of 15.00° and 38.16°; *i.e.* the (dibenzo-18-crown-6)K$^+$ complex is not symmetrical.

In contrast to **3**, two (dibenzo-18-crown-6)K$^+$ units form a dimeric structure involving K$^+$–π interactions between the K$^+$ ion of one unit and one aromatic ring of the adjacent moiety (see Fig. 14). The average distance between one K$^+$ cation and the mean plane of phenyl ring on the adjacent ligand of dibenzo-18-crown-6 is 3.106 Å. Additionally, the dimeric (dibenzo-18-crown-6)K$^+$ complexes further assemble into one-dimensional infinite columns (see Fig. 14D–F).

Adjacent TCNQ units (A and B) form extended face-to-face π-stacked dimers (A···B), which further assemble into extended infinite columns generating parallel sheets throughout the structure separated by columns of dimeric (dibenzo-18-crown-6)K$^+$ dimers (see Fig. 15). The similarity of
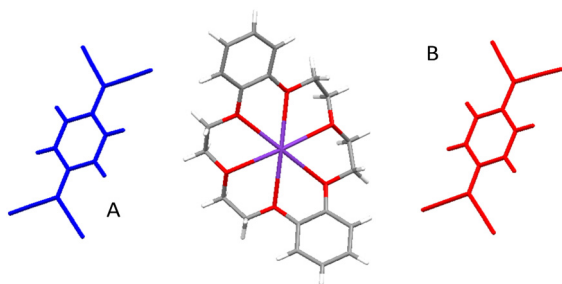
the bond lengths within the two TCNQ units makes it difficult to distinguish between the TCNQ$^{\cdot-}$ and TCNQ^0 components. Within each TCNQ dimer, individual TCNQ units are significantly long-axis slipped (see Fig. S4 and Table S2† for the key structural features) with a π–π separation of 3.123 Å. TCNQ-A is planar with both terminal –C(C≡N)$_2$ moieties slightly rotated in relation to the central aromatic ring (by 3.74° and 1.56°) whereas TCNQ-B units adopt a shallow boat conformation with both terminal –C(C≡N)$_2$ moieties slightly bent away (by 3.00° and 2.40°) from the benzenoid ring core.

Solid-state behaviour of (dicyclohexano-18-crown-6)K(TCNQ)$_3$ (5)

In the unit cell of (dicyclohexano-18-crown-6)K(TCNQ)$_3$ (**5**), the *cis–anti–cis* isomer of the dicyclohexano-18-crown-6 moiety occupies a crystallographic centre of symmetry. The six crown ether oxygen atoms form a nearly regular hexagon and thus outline a regular cavity. Each K$^+$ cation is coordinated by one crown ether ring and sited on the crystallographic centre of symmetry of the hexa-ether. The average distance of 2.799 Å between the K$^+$ cation and the crown ether oxygen atoms is identical to the value observed in the 1:1:1 complexes of dicyclohexano-18-crown-6 with potassium phenoxide and phenol.[31] Additionally, each K$^+$ ion is coordinated to two crystallographically equivalent TCNQ moieties (TCNQ-A and TCNQ-A') one on each face (see Fig. 16).

Fig. 13 "Butterfly" configuration adopted by the cation barrel of (dibenzo-18-crown-6)K$^+$ in **4** in this study.

Fig. 12 Asymmetric unit of (dibenzo-18-crown-6)K(TCNQ)$_2$ (**4**) in this study showing the two crystallographically inequivalent TCNQ units in different colours.
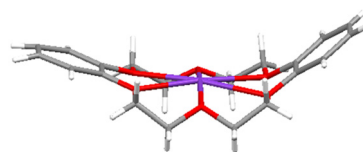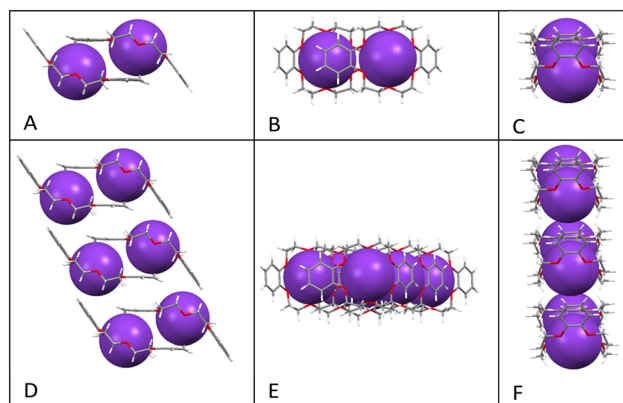

Fig. 14 Side (A/D), top (B/E), and end (C/F) views of dimeric configuration of cation barrel (dibenzo-18-crown-6)K$^+$ in **4** formed by inter-complex K$^+$–π interactions in this study.
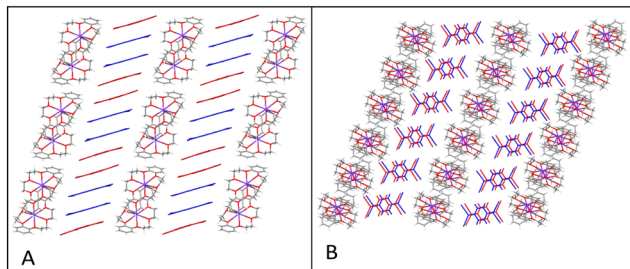
Fig. 15 Capped stick side (A) and top (B) views of packing motif in (dibenzo-18-crown-6)K(TCNQ)$_2$ (**4**) in this study.
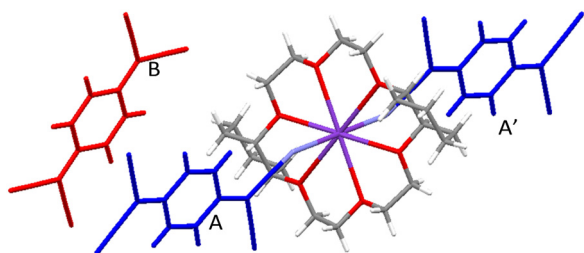
Fig. 16 The unit cell of (dicyclohexano-18-crown-6)K(TCNQ)$_3$ (**5**).
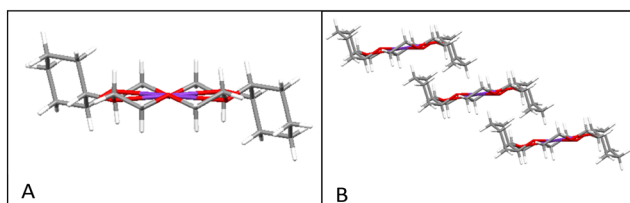
Fig. 17 Capped stick side view (A) and one-dimensional ladder conformation (B) formed by cation barrel of (dicyclohexano-18-crown-6)K$^+$ in **5**.

The (dicyclohexano-18-crown-6)K$^+$ complex adopts a chair conformation (see Fig. 17A). The angle between the cyclohexane ring best plane and the mean plane (as defined by six oxygen atoms) of the crown ether ring is 75.12°. Adjacent (dicyclohexano-18-crown-6)K$^+$ units form an infinite one-dimensional ladder with a centroid K$^+$–K$^+$ distance of 7.951 Å, and of 4.249 Å for the vertical distance between a K$^+$ cation and the mean plane (as defined by six oxygen atoms) of the neighbouring (dicyclohexano-18-crown-6)K$^+$ (see Fig. 17B).

Two of the adjacent TCNQ units (in blue in Fig. 18A), TCNQ-A and TCNQ-A′ form a TCNQ dimer which is significantly long-axis slipped (see Fig. S5 and Table S2† for the key structural features). The individual units of TCNQ-A or TCNQ-A′ adopt a shallow boat conformation, in which one terminal –C(C≡N)$_2$ moiety is bent slightly away (by 4.28°) from the plane of the central aromatic ring. On the other hand, TCNQ-B (red in Fig. 18A) adopts a planar conformation with the –C(C≡N)$_2$ moieties at both ends slightly twisted (2.52°) relative to the central benzenoid ring plane. Additionally, each TCNQ (blue) dimer (A···A′) is separated by
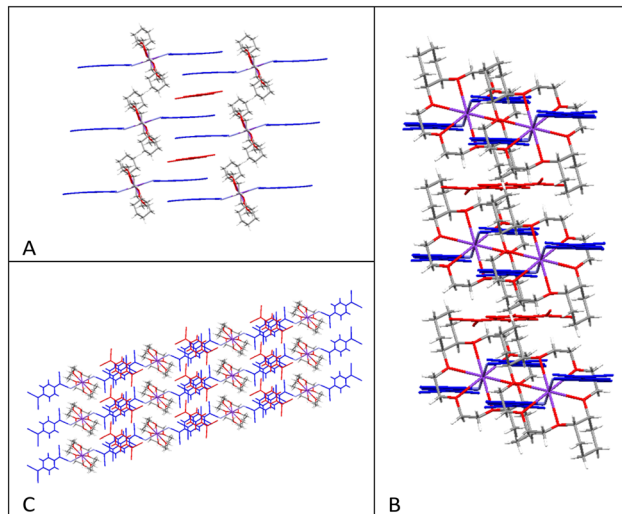
Fig. 18 Capped stick side (A), end (B), and top (C) views of the packing arrangement found in (dicyclohexano-18-crown-6)K(TCNQ)$_3$ (**5**).

a single (red) TCNQ-B unit (see Fig. 18). The TCNQ-B unit is rotated by 66.52° with respect to the TCNQ dimers. The packing motif of AA′BAA′ further assembles into infinite TCNQ columns. Meanwhile, the similarity of the bond lengths within TCNQ units makes it difficult to distinguish between the TCNQ$^{•-}$ and TCNQ^0 components.

Vibrational spectra of ionophore-encapsulated KTCNQ complexes (1–5)

Vibrational spectroscopy provides a valuable insight into the degree of charge transfer for the TCNQ species.[32] Table 1 presents key data for KTCNQ complexes (**1–5**) together with corresponding literature data for comparison. The infrared (IR) spectroscopy confirms that all of the KTCNQ complexes (**1–5**) in this study contain partially charged TCNQ species with stretching bands in the range between 2226 cm^{-1} to 2154 cm^{-1}, which are ascribed to –C≡N cyano groups. Meanwhile, the observed values of other –C≡C– stretching bands at ~1515 cm^{-1} indicate the mixed valence of TCNQ species (TCNQ$^{•-}$ and TCNQ^0 components). Stretching bands representing the –C≡N and –C≡C– groups are easily observed in Raman spectra because of the strongly polarizable π-electrons.[33] For all of the KTCNQ complexes (**1–5**), peaks in the range between 2207 cm^{-1} and 2197 cm^{-1} are ascribed to the cyano groups.[33] Meanwhile, the peaks observed between 1434 cm^{-1} and 1386 cm^{-1} are intermediate between those expected for TCNQ^0 and for TCNQ$^{•-}$, indicating a fractionally charged TCNQ unit in the solid-state architectures of all the KTCNQ complexes (**1–5**) reported in this study.[29,33,34]

Resistivity study of ionophore encapsulated KTCNQ complexes (1–5)

Resistivity measurements were carried out on compressed circle discs for all the KTCNQ complexes (**1–5**) at room

Table 1 IR and Raman data for the TCNQ complexes (**1**–**5**) together with selected comparative literature data

Compound	Infrared data/cm^{-1}		Raman data/cm^{-1}			Ref.
	C≡N stretch	C=C stretch	C≡N stretch	C=C stretch	C–C≡N stretch	
TCNQ^0	2228, 2225	1545	2225	1600	1450	30
TCNQ^0	2224, 2220	1545	2230	1603	1454	This work
KTCNQ	2215, 2162	1505				This work
1	2209, 2196, 2176	1522	2203	1603	1386	This work
2	2196, 2178,	1525	2189	1614, 1600	1434, 1389	This work
3	2226, 2195, 2166	1507	2207	1606	1390	This work
4	2214, 2189	1528	2204	1605	1388	This work
5	2222, 2201, 2174	1507	2203	1605	1389	This work
6	2201, 2187, 2177, 2158	1505	2197	1603	1388	7
7	2202, 2183, 2154	1508				1

Table 2 Resistivity data (as compressed powders) for ionophore–encapsulated KTCNQ salt (**1**–**5**) together with selected comparative literature values

Complex	Resistivity (Ω cm)	Ref.
KTCNQ	2.0×10^6	35
(15-Crown-5)$_m$(KTCNQ)$_n$	8.5×10^{11}	27, 36
(18-Crown-6)$_m$(KTCNQ)$_n$	6.7×10^9	27
([2.2.2]-Cryptand)$_m$(KTCNQ)$_n$	1.3×10^{10}	27, 36
(Dibenzo-18-crown-6)$_m$(KTCNQ)$_n$	$>10^{14}$	27
(Dibenzo-18-crown-6)$_m$(KTCNQ)$_n$TCNQ^0	4.4×10^3	27
1	2.6×10^7	This work
2	2.5×10^7	This work
3	4.7×10^5	This work
4	9.1×10^5	This work
5	$>2.0 \times 10^7$	This work

temperature. Table 2 illustrates the values of resistivity for all the KTCNQ complexes (**1**–**5**) together with corresponding literature data for comparison. Nogami and coworkers[27,36] have previously reported resistivity values for several KTCNQ complexes (see Table 2). The data in Table 2 shows that the observed resistivity values for all the KTCNQ complexes (**1**–**5**) and for (dibenzo-18-crown-6)$_m$(KTCNQ)$_n$(TCNQ^0)[27] are much lower than those of the corresponding simple salts (*i.e.* those without TCNQ^0 present) as expected.[27]

Preliminary electron paramagnetic resonance of ionophore encapsulated KTCNQ complexes (1 and 2)

The EPR behaviour of single crystals of both KTCNQ complexes, **1** and **2**, has been explored and compared with that of (18-crown-6)KTCNQ (**6**). In both **1** and **2**, only a central peak is observed which in the case of **2** shows some weak anisotropy (Fig. 19 shows EPR results for **1**). No additional signals were detected in scans up to 100 mT in width at 380 K at this and other crystal orientations. This is consistent with our previous observations for (15-crown-5)Li(TCNQ)$_2$·H$_2$O and (15-crown-5)Na(TCNQ)$_2$·H$_2$O[7] respectively. Furthermore, in **1**, the observed central peak signal intensity decreases with increasing temperature. This phenomenon is in agreement with the presence of a ground state doublet spin system obeying the Curie law,[7] which is in marked contrast with that seen for (18-crown-6)KTCNQ **6** (ref. 3) (see Fig. S6†). In **6**, because of the tilt angle between TCNQ dimers in

neighbouring columns, two independent spectral doublets are observed which show strong orientation dependence arising from the dipolar fine structure (zero-field splitting) of a triplet exciton state. The signal intensity of thermally populated triplet excitons such as those in **6** is increased at higher temperatures.[3]

The EPR properties of **2** at 295 K show no evidence for the observation of a localized triplet excited state at this temperature (see Fig. S7†). This preliminary finding is consistent with other complex TCNQ salts, which have extended mixed-valence columns of TCNQ species (*i.e.* containing both TCNQ$^{·-}$ and TCNQ^0 components).

Conclusions

In this study, we have prepared and structurally characterized by single crystal X-ray crystallography five ionophore-encapsulated "complex" KTCNQ salts: (18-crown-6)K(TCNQ)$_{2.5}$ (**1**), ([2.2.2]-cryptand)K(TCNQ)$_{2.5}$ (**2**), (benzo-18-crown-6)K(TCNQ)$_2$ (**3**), (dibenzo-18-crown-6)K(TCNQ)$_2$ (**4**), and (dicyclohexano-18-crown-6)K(TCNQ)$_3$ (**5**), respectively. Both **1** and **2** were obtained as unusual 2 : 5 (cation : TCNQ) ratio salts in which the K$^+$ cation sits within the cavity of the crown ether or [2.2.2]-cryptand. Additionally, the TCNQ components form pentamers as the repeating unit, which further assemble into infinite face-to-face π-stacked TCNQ columns with the corresponding cation barrels of (18-crown-6)K$^+$ or ([2.2.2]-cryptand)K$^+$ sitting in the cavities on either
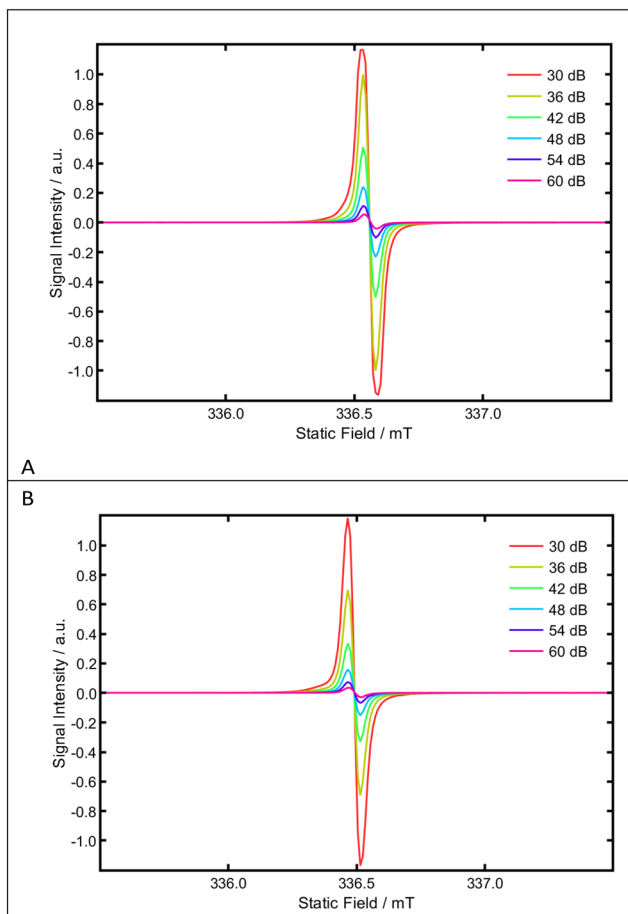
Fig. 19 Preliminary EPR analysis of **1** showing power saturation behaviour at (A) 295 K and (B) 380 K with microwave attenuation as indicated. Signal intensity is in the linear regime (double intensity for 6 dB increase in power) for attenuations of 36 dB or more (power 50 μW or less) at both temperatures, with a clear reduction in signal intensity at the higher temperature showing that the Curie law is obeyed.

side of the extended TCNQ columns. Furthermore, the TCNQ units form delocalized π-stacks within each repetitive penta-mer moiety. In both **3** and **4**, neighbouring (crown ether)K$^+$ complexes associate through K$^+$–π interactions. In the case of **3**, these cation barrels assemble into one-dimensional infinite stacks whereas in **4**, neighbouring (dibenzo-18-crown-6)K$^+$ complexes form a dimeric structure. The TCNQ units form dimers, which are further assembled into infinite columns with the corresponding (crown ether)K$^+$ complexes fitting into the cavities between the extended TCNQ columns. Again, the electrons are delocalized within the TCNQ units. In **5**, the crown ether ring adopts a "chair" conformation, in which the K$^+$ cation is sitting in the geometric centre and coordinated by one crown ether ligand and two cyano groups on adjacent TCNQ units. In the solid-state, neighbouring TCNQ dimers are separated by an isolated TCNQ unit resulting in the formation of infinite TCNQ columns which sit between the sheets of the (dicyclohexano-18-crown-6)K$^+$ complexes. Vibrational spectroscopic data are consistent with

the partially charged nature of the TCNQ species in all the KTCNQ complexes (**1–5**). Resistivity measurements demonstrate that all the KTCNQ complexes (**1–5**) have a relatively higher conductivity compared with the corresponding simple KTCNQ salts (*i.e.* without TCNQ^0 present). Preliminary EPR analysis of **1** and **2** reveals that there is no evidence for localized triplet excited states, which is in agreement with the presence of extended mixed TCNQ stacks in complex TCNQ salts. Whilst in complexes **1** and **5** the TCNQ units co-ordinate directly with the cation, in the remaining complexes there is no direct association. Indeed in structures **3** and **4** cation–π interactions appear to play a key role in the solid-state behaviour. There are currently very few examples of complex TCNQ salts which do not involve metal ion–TCNQ coordination and the results presented here may provide new routes to exploring through-space interactions between metal ions and complex TCNQ salts in the solid state.

Conflicts of interest

There are no conflicts to declare.

Acknowledgements

References

1 M. C. Grossel and S. C. Weston, *Chem. Mater.*, 1996, **8**, 977–980.
2 M. C. Grossel, F. A. Evans, J. A. Hriljac, K. Prout and S. C. Weston, *J. Chem. Soc., Chem. Commun.*, 1990, 1494–1495.
3 R. C. Hynes, J. R. Morton, K. F. Preston, A. J. Williams, F. Evans, M. C. Grossel, L. H. Sutcliffe and S. C. Weston, *J. Chem. Soc., Faraday Trans.*, 1991, **87**, 2229–2233.
4 M. C. Grossel and S. C. Weston, *J. Phys. Org. Chem.*, 1992, **5**, 533–539.
5 M. C. Grossel, F. A. Evans, J. A. Hriljac, J. R. Morton, Y. Lepage, K. F. Preston, L. H. Sutcliffe and A. J. Williams, *J. Chem. Soc., Chem. Commun.*, 1990, 439–441.
6 M. C. Grossel and S. C. Weston, *J. Chem. Soc., Chem. Commun.*, 1992, 1510–1512.
7 B. Yan, P. N. Horton, A. E. Russell, C. J. Wedge, S. C. Weston and M. C. Grossel, *CrystEngComm*, 2019, **21**, 3273–3279.
8 R. M. Izatt, J. S. Bradshaw, S. A. Nielsen, J. D. Lamb, J. J. Christensen and D. Sen, *Chem. Rev.*, 1985, **85**, 271–339.
9 R. M. Izatt, K. Pawlak, J. S. Bradshaw and R. L. Bruening, *Chem. Rev.*, 1991, **91**, 1721–2085.
10 R. M. Izatt, K. Pawlak, J. S. Bradshaw and R. L. Bruening, *Chem. Rev.*, 1995, **95**, 2529–2586.
11 Y. Zhu, J. Dou, D. Li and D. Wang, *Indian J. Chem., Sect. A: Inorg., Bio-inorg., Phys., Theor. Anal. Chem.*, 2004, **43**, 2126–2131.

12 F. R. Fronczek, R. D. Gandour, L. M. Gehrig, L. R. Caswell, K. A. McDowell and I. Alam, *J. Inclusion Phenom. Macrocyclic Chem.*, 1987, **5**, 379–383.

13 G. W. Gokel, W. M. Leevy and M. E. Weber, *Chem. Rev.*, 2004, **104**, 2723–2750.

14 S. Yamaguchi, S. Akiyama and K. Tamao, *Organometallics*, 1999, **18**, 2851–2854.

15 M. R. MacDonald, M. E. Fieser, J. E. Bates, J. W. Ziller, F. Furche and W. J. Evans, *J. Am. Chem. Soc.*, 2013, **135**, 13310–13313.

16 J. Lu, X. Qu, G. Peleckis, J. F. Boas, A. M. Bond and L. L. Martin, *J. Org. Chem.*, 2011, **76**, 10078–10082.

17 J. Huang, S. Kingsbury and M. Kertesz, *Phys. Chem. Chem. Phys.*, 2008, **10**, 2625–2635.

18 K. Sambe, N. Hoshino, T. Takeda, T. Nakamura and T. Akutagawa, *Cryst. Growth Des.*, 2020, **20**, 3625–3634.

19 K. Sambe, N. Hoshino, T. Takeda, T. Nakamura and T. Akutagawa, *J. Phys. Chem. C*, 2020, **124**, 13560–13571.

20 S. J. Coles and P. A. Gale, *Chem. Sci.*, 2012, **3**, 683–689.

21 *CrystalClear*, Rigaku Corporation, The Woodlands, Texas, U.S.A., 2008–2014.

22 *CrysAlisPro Software System*, Rigaku Oxford Diffraction, 2021.

23 O. V. Dolomanov, L. J. Bourhis, R. J. Gildea, J. A. Howard and H. Puschmann, *J. Appl. Crystallogr.*, 2009, **42**, 339–341.

24 G. M. Sheldrick, *Acta Crystallogr., Sect. A: Found. Adv.*, 2015, **71**, 3–8.

25 G. M. Sheldrick, *Acta Crystallogr., Sect. C: Struct. Chem.*, 2015, **71**, 3–8.

26 G. R. Desiraju, *Angew. Chem., Int. Ed. Engl.*, 1995, **34**, 2311–2327.

27 M. Morinaga, T. Nogami, Y. Kanda, T. Matsumoto, K. Matsuoka and H. Mikawa, *Bull. Chem. Soc. Jpn.*, 1980, **53**, 1221–1227.

28 S. C. Weston, *PhD thesis*, University of London, 1992.

29 F. H. Herbstein and M. Kapon, *Crystallogr. Rev.*, 2008, **14**, 3–74.

30 T. Takenaka, *Bull. Inst. Chem. Res., Kyoto Univ.*, 1969, **47**, 387–400.

31 M. E. Fraser, S. Fortier, M. K. Markiewicz, A. Rodrigue and J. W. Bovenkamp, *Can. J. Chem.*, 1987, **65**, 2558–2563.

32 Z. Zhang, H. Zhao, M. M. Matsushita, K. Awaga and K. R. Dunbar, *J. Mater. Chem. C*, 2014, **2**, 399–404.

33 E. Faulques, A. Leblanc, P. Molinié, M. Decoster, F. Conan, J. Guerchais and J. Sala-Pala, *Spectrochim. Acta, Part A*, 1995, **51**, 805–819.

34 C. Ye, G. Cao, F. Fang, H. Xu, X. Xing, D. Sun and G. Chen, *Micron*, 2005, **36**, 461–464.

35 H. H. Afify, F. M. Abdel-Kerim, H. F. Aly and A. A. Shabaka, *Z. Naturforsch.*, 1978, **33**, 344–346.

36 T. Nogami, M. Morinaga, Y. Kanda and H. Mikawa, *Chem. Lett.*, 1979, **8**, 111–112.